

Suicide inactivation of xanthine oxidoreductase during reduction of inorganic nitrite to nitric oxide

Ben L. J. GODBER, Justin J. DOEL, Tracey A. GOULT, Robert EISENTHAL and Roger HARRISON¹

Department of Biology and Biochemistry, University of Bath, Claverton Down, Bath BA2 7AY, U.K.

Xanthine oxidoreductase (XOR) is progressively inactivated while catalysing the reduction of inorganic nitrite to NO by xanthine. Inactivation results from conversion of the enzyme into its desulpho-form. The rate of inactivation increases with nitrite concentration. Similar behaviour was shown when NADH replaced xanthine as reducing substrate. A kinetic model is proposed incorporating a 'suicide' inactivation involving an enzyme–substrate (product) complex, rather than inactivation by free NO. The model provides a good fit to progress curves of the reaction of xanthine or NADH with nitrite in the presence of

the oxidase or dehydrogenase forms of the enzyme. Inorganic nitrate, like nitrite, was shown to be reduced at the molybdenum site of XOR. With xanthine as reducing substrate, nitrite was produced in essentially a 1 : 1 stoichiometric ratio with respect to urate. Unlike the case of nitrite, the enzyme was not significantly inactivated, implying that inactivation during nitrite reduction depends on the presence of nascent NO in its enzyme complex.

Key words: sulpho-desulpho conversion, xanthine dehydrogenase, xanthine oxidase.

INTRODUCTION

The molybdoflavoenzyme, xanthine oxidoreductase (XOR), occurs widely in Nature, and has been studied intensively [1], being readily available in cows' milk, where it is a major protein component of the milk fat globule membrane [2,3]. XOR occurs as a homodimer; each 147 kDa subunit contains one molybdenum atom, one FAD and two Fe₂S₂ centres [2,4]. In mammals, XOR exists in two interconvertible forms, xanthine dehydrogenase (XDH; EC 1.1.1.204), which predominates *in vivo*, and xanthine oxidase (XO; EC 1.1.3.22). Both forms of the enzyme reduce molecular oxygen, although only XDH can reduce NAD⁺, which is its preferred electron acceptor. Reduction of oxygen yields superoxide anion and hydrogen peroxide, and it is the capacity to generate these reactive oxygen species that has focused attention on the enzyme in recent years [5–8].

In bovine milk, XOR commonly occurs in two 'inactive' forms that lack catalytic activity involving the molybdenum centre [2,4,9,10]. Demolybdo-XOR lacks the molybdenum atom and can make up as much as 40% of freshly purified enzyme [11–13]. Molybdenum-containing enzyme can itself contain 30–40% of a second inactive form, namely desulpho-XOR, in which a Mo=S grouping, essential for activity towards most reducing substrates, is replaced by Mo=O. The presence of these inactive forms has long been a puzzle and, while different contents of molybdenum have been attributed to nutritional variation [14], the origins and physiological significance of both forms, particularly desulpho-XOR, remain a topic for debate [7].

NO is a biological messenger, known to be involved in a wide range of physiological processes [15,16], and generally accepted to arise *in vivo* from the enzyme NO synthase [17]. We have recently reported that NO can also result from the reduction of nitrites, both inorganic [18,19] and organic [20], catalysed by XOR. NO is known to inhibit the activity of several enzymes, including aconitase [21], glutathione peroxidase [22], cytochrome *c* oxidase [23,24] and NADPH oxidase [25]. More recently,

attention has been directed to XOR, effective concentrations of which are increased in a number of pathological conditions that also involve increased rates of NO production [26–29]. In the case of XOR, however, reported results have proved to be highly controversial. Initial reports of NO-induced inhibition of XOR, in cell-free conditions [30], interferon- γ -stimulated macrophages [31] and endothelial cells [32,33], have been followed by both negative [34,35] and positive [36] findings obtained with purified enzyme.

Ichimori et al. [36] reported that NO inactivates purified bovine milk XOR, under anaerobic conditions and in the presence of xanthine, by conversion into its desulpho-form. In the course of XOR-catalysed reduction of inorganic nitrite to NO under anaerobic conditions we observed progressive inactivation of the enzyme [18]. This appeared to be consistent with the findings of Ichimori et al. [36], and indeed we showed that our inactivated enzyme could be reactivated by standard re-sulphuration procedures [18]. We have re-examined the mechanisms of inactivation of XOR during the enzyme-catalysed reduction of inorganic nitrite to NO under anaerobic conditions. Kinetic analysis is consistent with a rapid inactivation of the enzyme at the stage of its complex with substrate/product. Inactivation by free NO, as described by Ichimori et al. [36], if occurring, is a very much slower process in this system.

EXPERIMENTAL

XO and XDH

XO was purified from bovine milk and stored at -70°C as described by Godber et al. [18]. The enzyme showed an A_{280}/A_{450} value of 5.0–5.2 and, following thawing, contained $>97\%$ oxidase activity, as determined by the method described below. The enzyme contained 35–38% functional active sites, as judged by activity-to-flavin ratio (AFR), assuming that fully active enzyme has a ratio of 208 [37].

Abbreviations used: XOR, xanthine oxidoreductase; XO, xanthine oxidase; XDH, xanthine dehydrogenase; IoDP, iodonium diphenyl.

¹ To whom correspondence should be addressed (e-mail bssrh@bath.ac.uk).

XDH was prepared by incubating XO in the presence of 10 mM dithiothreitol at 37.0 ± 0.2 °C for 1 h, followed by gel filtration on a PD-10 desalting column (Pharmacia). XDH prepared in this manner contained 10–15% oxidase activity, as determined by the method described below.

Concentrations of enzyme were determined from the UV-visible spectrum, by using an absorption coefficient of 36 mM^{-1} (of subunit) $\cdot \text{cm}^{-1}$ at 450 nm [2]. The oxidase contents of XO or XDH were determined by measuring the rate of oxidation of xanthine to uric acid spectrophotometrically at 295 nm in a Cary 100 spectrophotometer, using an absorption coefficient of $9.6 \text{ mM}^{-1} \cdot \text{cm}^{-1}$ [38]. Assays were performed at 25.0 ± 0.2 °C in air-saturated Na-Bicine buffer, pH 8.3, containing 100 μM xanthine. The sum of oxidase and dehydrogenase contents was determined as above but in the presence of 0.5 mM NAD^+ .

Iodonium diphenyl (IoDP)-inhibited enzyme

IoDP-inhibited XO was prepared essentially as described by O'Donnell et al. [39] and outlined by Godber et al. [18].

Reagents

Dithiothreitol was purchased from Alexis Corp. Oxygen-free nitrogen and compressed air were from British Oxygen Corp. All other reagents, unless otherwise stated, were purchased from Sigma.

Kinetics of XOR-catalysed oxidation of xanthine or NADH in the presence of inorganic nitrite or nitrate

All kinetic studies were carried out under anaerobic conditions in nitrogen-sparged 50 mM potassium phosphate buffer, pH 7.2, at 25.0 ± 0.2 °C using an anaerobic cabinet (Belle Technologies) containing < 3 p.p.m. O_2 . XOR was mixed with 100 μM xanthine or 100 μM NADH and various concentrations of sodium nitrite or nitrate, using a Hi-Tech SF61 rapid-mixing device. With xanthine as reducing substrate, urate was determined as described above for determination of oxidase content of XOR. With NADH as reducing substrate, NADH utilization was followed at 340 nm using an absorption coefficient of $6.22 \text{ mM}^{-1} \cdot \text{cm}^{-1}$ [40].

Fluorescence assay for XOR activity

The sensitive assay of Beckman et al. [41] was used for samples with low XOR activity. The assay utilizes the enzyme-catalysed oxidation of pterin to isoxanthopterin, an oxidation totally analogous to that of xanthine to urate. Assays were carried out in a Perkin-Elmer LS-50B luminescence spectrometer at 25.0 ± 0.2 °C, and isoxanthopterin was detected fluorimetrically with an excitation wavelength of 345 nm and emission wavelength of 390 nm. Sample was added to 50 mM potassium phosphate, pH 7.2, in 1 ml quartz fluorimeter cells and fluorescence was monitored to ensure a stable baseline. Pterin was added to a final concentration of 10 μM , mixed by inversion and the rate of fluorescence change was determined. Confirmation that the generation of product was allopurinol-inhibitable was obtained by addition of allopurinol to a final concentration of 10 μM . The system was calibrated by adding known amounts of isoxanthopterin, which acts as an internal standard and takes into account the differences observed in fluorescence quenching and light scatter.

Inactivation of XOR in the presence of inorganic nitrite or nitrate

XOR was incubated in an anaerobic cabinet, as described above, with various concentrations of sodium nitrite or nitrate and xanthine. Aliquots (400 μl) of the reaction mixture were taken at intervals, gel filtered on a PD-10 desalting column (Pharmacia) and assayed fluorimetrically for enzyme activity, as described above. In larger-scale experiments, where spectral changes of the enzyme were also monitored, the spectrophotometric urate assay was used (see above). These latter experiments were carried out at 20 °C to allow sufficient time to record enzyme activities and spectra. As the enzyme concentrations in the PD-10 eluates were not identical, the spectra were normalized using the ratio of the absorbances at 450 and 650 nm.

UV-visible spectra of XO before and after inactivation

XO (2.1 μM) was incubated under anaerobic conditions (see above) for 1 h, in the absence and presence of 1 mM xanthine and 80 mM sodium nitrite. Samples of enzyme were gel filtered to remove substrates and product and the UV-visible spectra were recorded using a Cary 100 spectrometer. XO incubated in the absence and presence of xanthine and sodium nitrite showed specific activities of 1620 and 48 nmol of urate $\cdot \text{min}^{-1} \cdot \text{mg}^{-1}$ respectively, the latter representing 3% of the former.

Use of NO electrode for inhibition kinetics

NO was measured by using a specific electrode (ISO-NO World Precision Instruments) in a water-jacketed, stirred chamber. The tip of the electrode was submerged 5 mm into the reaction buffer. Reactions (4 ml) were carried out in nitrogen-sparged 50 mM potassium phosphate, pH 7.2, at 25.0 ± 0.2 °C in an anaerobic cabinet and started by addition of enzyme. Readings of current were taken at 5 s intervals and plotted against time to obtain initial rates. The electrode was calibrated under the conditions of the assay by using a standard NO-generating system (ISO-NO Technical Manual), whereby known quantities of sodium nitrite were added to 0.1 M sulphuric acid, containing 0.1 M potassium iodide, to give stoichiometric amounts of NO. Recorded currents were plotted against concentrations of NO to give a linear standard curve.

Determination of nitrite concentrations

Nitrite concentrations were determined by using the Griess reagent system (Promega, Madison, WI, U.S.A.), which relies on a diazotization reaction between sulphanilamide and *N*-1-naphthylethylenediamine dihydrochloride under acid conditions [42]. In the presence of nitrite, a magenta colour develops which is monitored at 535 nm. Nitrite concentration was determined from a standard reference curve in the range 0–200 μM .

Analysis of kinetic data

The fitting of the kinetic model of Scheme 1 (see below) to time courses of inactivation and to progress curves was carried out using Scientist software (MicroMath), employing non-linear least-squares minimization of the numerically integrated rate equations utilizing Powell's algorithm. Characterization of steady-state inhibition was carried out using the complementary methods of Dixon [43] and Cornish-Bowden [44].

RESULTS

In the presence of nitrite and xanthine, XO is progressively inactivated by conversion into its desulpho-form

We have previously reported that the incubation of XO with inorganic nitrite and xanthine under anaerobic conditions generates NO and that the enzyme is progressively inactivated [18]. After prolonged incubation, XO was shown to have been converted into its desulpho-form. This was demonstrated by its reactivation under standard resulphuration conditions, involving anaerobic incubation of dithionite-reduced enzyme with sulphide [18]. That the inactivated enzyme, so obtained, was indeed desulpho-XO was confirmed by determination of its UV-visible spectrum (Figure 1), which is characteristic of this form [45]. As noted previously [45], the difference spectrum between desulpho- and sulpho-XO shows two minima, at 320 and 437 nm. Monitoring of absorbance changes at 320 nm allowed the sulpho-desulpho conversion to be followed during the course of incubation of XO with xanthine and nitrite. By these means, the conversion was shown to be concurrent with inactivation of the enzyme (Figure 2).

Dependence of XO inactivation rate on nitrite concentration

In order to clarify the mechanisms underlying the above inactivation, the loss of enzyme activity was followed over time at various initial nitrite concentrations. The results are shown in Figure 3, in which it is seen that the rate of activity loss increases with increasing nitrite concentration.

Two kinetic mechanisms can be proposed that might account for the above inactivation. The first is based on the findings of Ichimori et al. [36], who reported that XO activity of XOR is abolished during incubation of the enzyme with NO. These workers found that the kinetics of inactivation were pseudo first order in enzyme, with a second-order rate constant of $14.8 \text{ M}^{-1} \cdot \text{s}^{-1}$. They also proposed that inactivation only occurs in the presence of reducing substrate and in the absence of oxygen, implying that the inactivation process involves a reduced

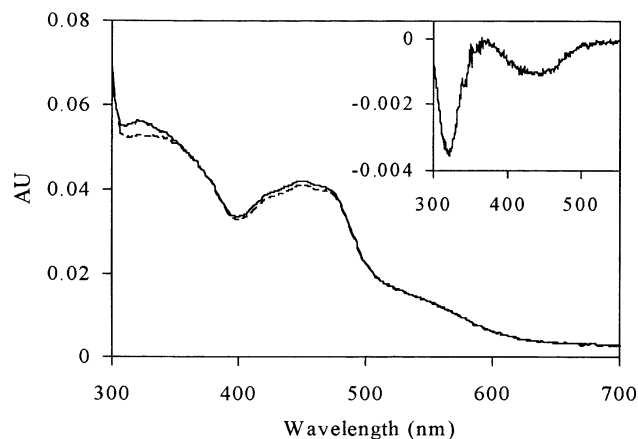


Figure 1 UV-visible spectra of XO (solid line) and inactivated XO after incubation in the presence of xanthine and NaNO_2 (broken line)

XO was incubated under anaerobic conditions in the absence and presence of xanthine and sodium nitrite. The difference spectrum, obtained by subtracting the spectrum of the inactivated XO from that of the active enzyme is shown in the inset.

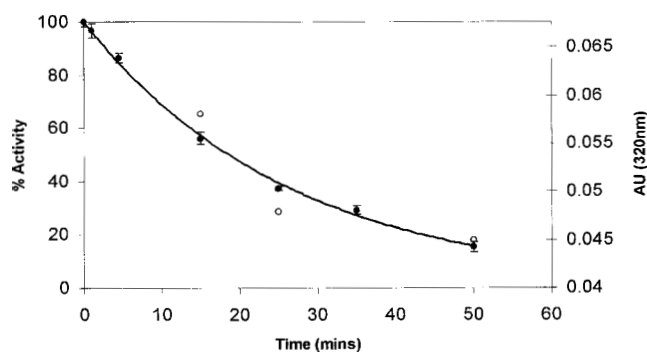


Figure 2 Correlation of rate of decay of XO enzymic activity with sulpho-desulpho conversion

XO ($6 \mu\text{M}$ active subunits) was incubated under anaerobic conditions with 1 mM xanthine and 50 mM sodium nitrite. ●, Percentage initial enzyme activity; ○, absorbance at 320 nm. The solid line represents the fit of enzyme activity measurements to a first-order decay curve.

species of XOR. In the current study, NO generated during the incubation [18] could then inactivate reduced enzyme. This mechanism can be formulated as a two-stage process where $\text{E} + \text{S} \leftrightarrow \text{ES} \rightarrow \text{E} + \text{P}$ occurs concurrently with $\text{E} + \text{P} \rightarrow \text{E}_x$ where E_x is inactivated enzyme. Such a mechanism would be expected to show a lag in the inactivation process, as the product concentration increases with time. Attempts to fit this mechanism to the activity decay data (Figure 3, dashed lines) do indeed display a sigmoid shape. As can be seen, the fit is poor.

A possible alternative is based on a mechanism-induced inactivation process (sometimes termed 'suicide' inactivation). This would occur in the enzyme-substrate (or enzyme-product) complex during turnover of substrate to product. At any fixed substrate concentration (i.e. assuming no substrate depletion), such a mechanism would be expected to show a simple monotonic exponential decay of activity with time.

The good fits of the experimental data to monotonic decay curves (Figure 3) suggest that a suicide mechanism of inactivation is likely. However, it is possible that there is a contribution from the product-based inactivation process, giving rise to a small initial lag in the inactivation curve. Such a small lag might be missed because of potential inaccuracies at early time points, resulting from the need to gel filter samples prior to assay of remaining enzyme activity. Gel filtering is necessary to avoid reaction of residual NO with superoxide, generated in the aerobic assay, to give peroxynitrite and consequent further inactivation [34,35].

Progress curves of XOR-catalysed oxidation of xanthine in the presence of nitrite

Confirmation of the existence of the suicide mechanism was sought from kinetic analysis of the progress curves for the enzyme-catalysed anaerobic reduction of nitrite to NO by xanthine. Such analysis should provide independent evidence for the suicide mechanism, and also allow quantitative assessment of the contribution of each of the two mechanisms to the inactivation process, as well as supplying accurate estimates of the kinetic parameters involved.

A minimal kinetic model for the XOR-catalysed reduction of inorganic nitrite, which incorporates both inactivation by product and suicide inactivation, is shown in Scheme 1. Here, E_{ox}

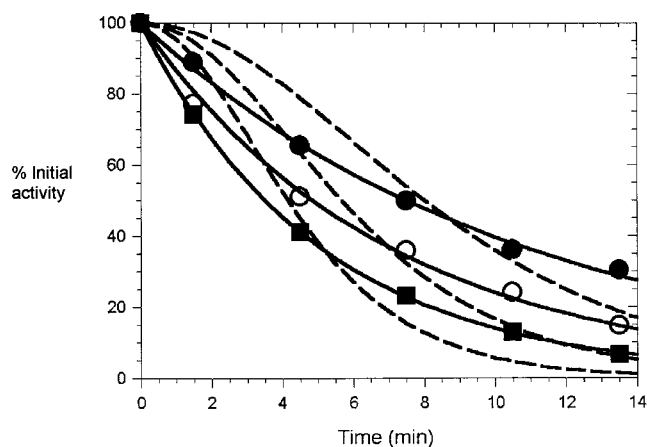
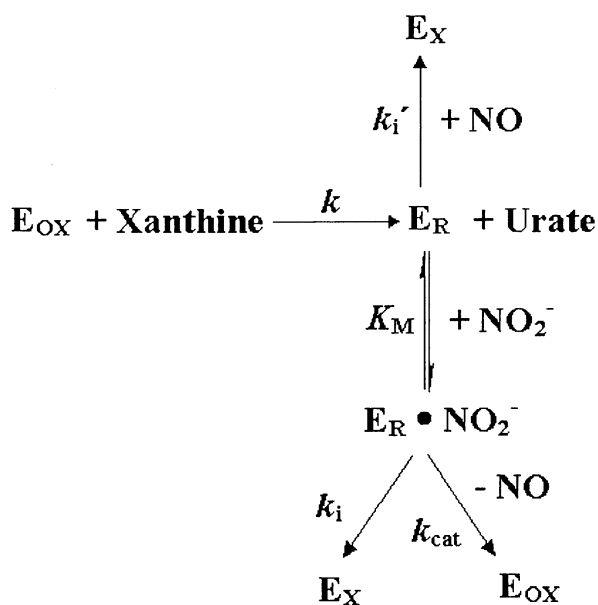


Figure 3 Dependence of decay of enzymic activity on time and nitrite concentration

XO (10 nM active subunits) was incubated under anaerobic conditions with 100 μ M xanthine and 15 mM (●), 30 mM (○) or 60 mM (■) sodium nitrite. The percentage of initial enzymic activity is plotted against time. Values are means \pm S.D. ($n = 3$) of samples taken from individual experiments. The solid lines represent the fits to a single exponential decay curve. Dashed lines are fits to a mechanism involving inactivation by accumulated product (see the Results section).



Scheme 1 A minimal kinetic model for the XOR-catalysed reduction of inorganic nitrite, incorporating both inactivation by product and suicide inactivation

E_{OX} , oxidized enzyme; E_R , reduced enzyme; E_X , inactivated enzyme; $\text{E}_R \cdot \text{NO}_2^-$ is the enzyme–substrate and/or enzyme–product complex.

represents oxidized enzyme, E_R is reduced enzyme and E_X is inactivated enzyme. $\text{E}_R \cdot \text{NO}_2^-$ is the enzyme–substrate and/or the enzyme–product complex. In this model, inorganic nitrite reacts with a reduced form of XO to yield an enzyme–substrate (or enzyme–product) complex. This can break down in two ways: productively, to yield product NO plus a (relatively) oxidized form of the enzyme or destructively, to give inactivated enzyme.

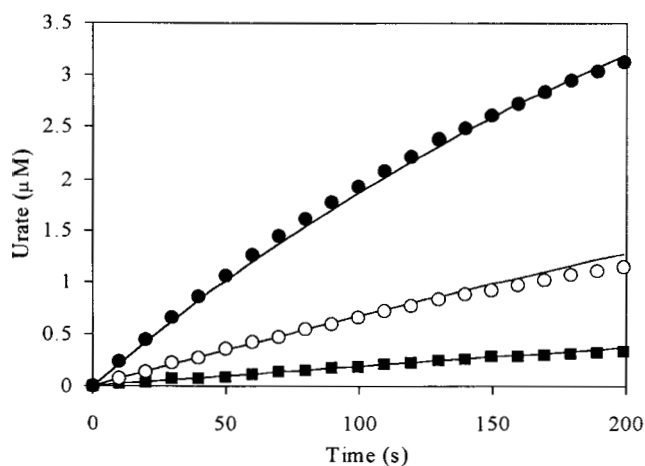


Figure 4 Progress curves of urate production catalysed by XO in the presence of xanthine and inorganic nitrite

XO (10.2 nM active subunits) was incubated anaerobically with xanthine and various concentrations of sodium nitrite: 120 mM (●), 30 mM (○) and 7.5 mM (■). Values are means from three individual progress curves. Solid lines represent fits to the model shown in Scheme 1, using the parameters shown in Table 1.

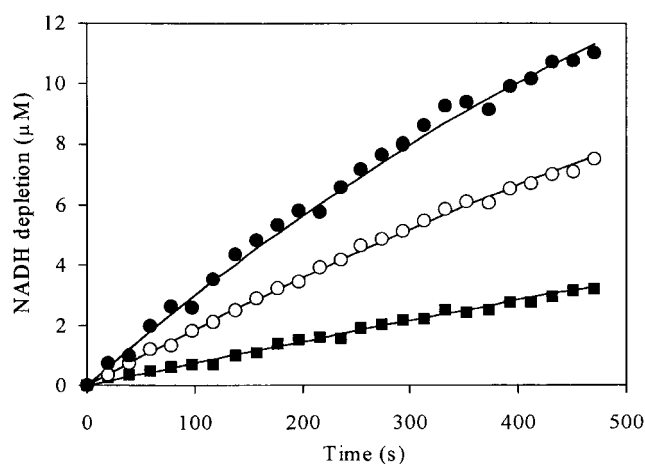


Figure 5 Progress curves of NADH depletion catalysed by XO in the presence of inorganic nitrite

XO (57.8 nM active subunits) was incubated anaerobically with NADH and various concentrations of sodium nitrite: 120 mM (●), 30 mM (○) and 7.5 mM (■). Values are means from three individual progress curves. Solid lines represent fits to the model shown in Scheme 1, using the parameters shown in Table 1.

In addition, the model incorporates a step that involves the inactivation of reduced enzyme by enzyme-generated free NO in a second-order reaction, as proposed by Ichimori et al. [36]. The model is defined by the following relationships, where E_T represents total enzyme concentration:

$$d[\text{urate}]/dt = k[\text{xanthine}] \quad (1)$$

$$[\text{E}_R \cdot \text{NO}_2^-] = [\text{NO}_2^-](\text{E}_T - [\text{E}_{OX}] - [\text{E}_X]) / (K_M + [\text{NO}_2^-]) \quad (2)$$

$$d[\text{E}_X]/dt = k_i[\text{E}_R \cdot \text{NO}_2^-] + k_1'[\text{NO}][\text{E}_R] \quad (3)$$

$$d[\text{E}_{OX}]/dt = k_{cat}[\text{E}_R \cdot \text{NO}_2^-] \quad (4)$$

Xanthine concentration was held constant at a value such that depletion of xanthine does not occur to any significant extent,

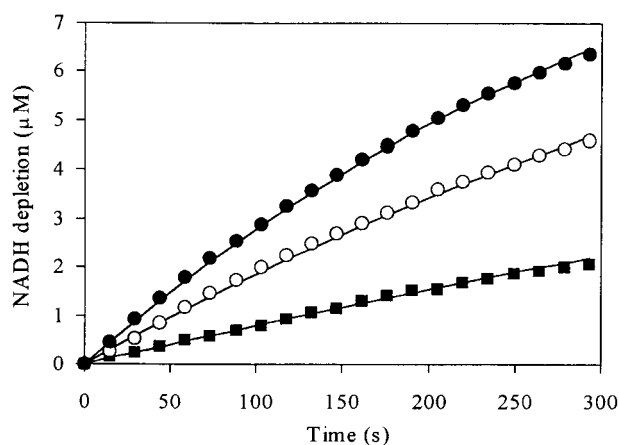


Figure 6 Progress curves of NADH depletion catalysed by XDH in the presence of inorganic nitrite

XDH (16.3 nM active subunits) was incubated anaerobically with NADH and various concentrations of sodium nitrite: 60 mM (●), 15 mM (○) and 3.75 mM (■). Values are means from three individual progress curves. Solid lines represent fits to the model shown in Scheme 1, using the parameters shown in Table 1.

justifying the first-order relationship for eqn (1), where k represents the operational rate constant under experimental conditions. The first-order rate constants, k_{cat} and k_1 , apply respectively to the productive and suicide reactions occurring on the enzyme–substrate–product complex. The second-order rate constant, k'_1 , is that of the product-driven inactivation step.

Progress curves for the XO-catalysed production of urate from 100 μM xanthine were recorded at 295 nm at three concentrations of inorganic nitrite. K_m and k_{cat} values were obtained from the initial linear rates. The value of k'_1 used was that of Ichimori et al. [36]; k was fixed at 100 000 s^{-1} , assuming that the xanthine/urate conversion is much faster than the reactions involving inorganic nitrite. The data and fitted curves are shown in Figure 4.

To assess the generality of the model, progress curves were determined for the XOR-catalysed reaction of nitrite with NADH, which has also been shown to produce NO [18]. Unlike the case with xanthine as reducing substrate, XO and XDH differ widely in their catalytic rates [18]; therefore, progress curves were obtained with both forms of the enzyme. The resulting data are shown in Figures 5 and 6, together with fits to the model. The suicide inactivation route, involving k_1 , is clearly dominant in that the contribution of k'_1 to inactivation was shown to be less than 0.7% of the total over the time course of Figure 4. The kinetic parameters resulting from the fits shown in Figures 4–6 are given in Table 1.

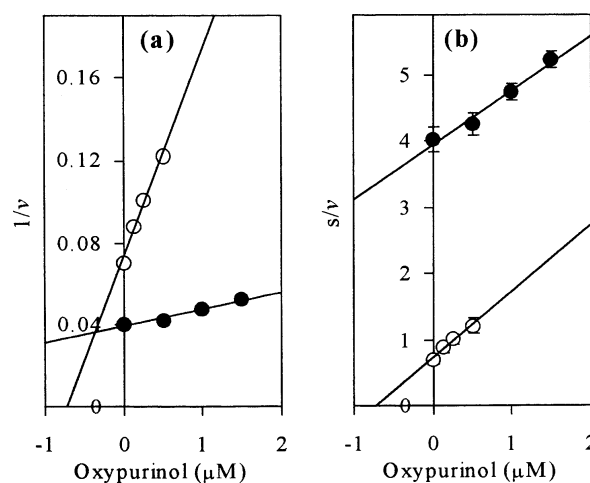


Figure 7 Inhibition by oxypurinol of NADH oxidation catalysed by XO in the presence of inorganic nitrate

XO (70 nM active subunits) was incubated under anaerobic conditions with 100 μM NADH and various concentrations of sodium nitrate and oxypurinol. The initial rate of NADH depletion (v) is expressed in $\text{nmol}\cdot\text{min}^{-1}\cdot\text{mg}^{-1}$. (a) Dixon plot [43] of $1/v$ versus concentration of oxypurinol at different concentrations of nitrate. (b) Cornish-Bowden plot [44] of s/v versus concentration of oxypurinol at different concentrations of nitrate. Concentrations of nitrate were 100 mM (●) and 10 mM (○). Both plots are diagnostic for simple competitive inhibition of oxypurinol against nitrate. Values are means \pm S.D. ($n = 3$).

XOR catalyses the reduction of inorganic nitrate at the molybdenum site

We sought to gain further information by examining the reduction of inorganic nitrate, which is also known to be reduced to NO [46] and for which the initial enzyme complex was expected to differ from that with inorganic nitrite. As in the case of inorganic nitrite [18], inorganic nitrate was shown to be reduced at the molybdenum site of the enzyme. This was evidenced by the fact that XO-catalysed oxidation of NADH in the presence of inorganic nitrate was competitively inhibited by oxypurinol (Figure 7), which binds to the reduced molybdenum site of the enzyme [18,37]. Moreover, oxidation of xanthine was shown to be unaffected (Figure 8) by treatment of XO with the FAD-site inhibitor, IoDP [18,39].

XO (660 nM active subunits) was incubated with 200 μM xanthine and 30 μM sodium nitrate, and urate production was monitored continuously at 295 nm, as described in the Experimental section. At different time intervals, aliquots (300 μl) were removed from the reaction vessel and the reaction was stopped by addition of 100 μM oxypurinol before assay of nitrite using the Griess reaction (see the Experimental section). Gen-

Table 1 Kinetic parameters used in the fits of the model of Scheme 1 to the progress curves shown in Figures 4, 5, 6 and 10

Values of K_m and k_{cat} were calculated from the initial rates of the progress curves assuming Michaelis–Menten kinetics and no initial inactivation. k'_1 is assigned the value found by Ichimori et al. [36]. Values of k_1 were obtained by fitting the model of Scheme 1 to the progress curves. Experimental conditions are described in the legends to Figures 4, 5, 6 and 10.

	K_m (mM)	k_{cat} (s^{-1})	k_1 (s^{-1})	k_{cat}/k_1	k'_1 ($\text{M}^{-1}\cdot\text{s}^{-1}$)
XO + xanthine + NaNO_2	280 ± 25	7.2 ± 0.6	0.012 ± 0.001	630 ± 92	14.8
XO + NADH + NaNO_2	33 ± 1.2	0.7 ± 0.02	0.0016 ± 0.002	450 ± 44	14.8
XDH + NADH + NaNO_2	14 ± 0.1	2.4 ± 0.03	0.0033 ± 0.001	740 ± 33	14.8
XO + xanthine + NaNO_3	48 ± 0.3	1.6 ± 0.04	0.0003 ± 0.0001	6100 ± 310	–

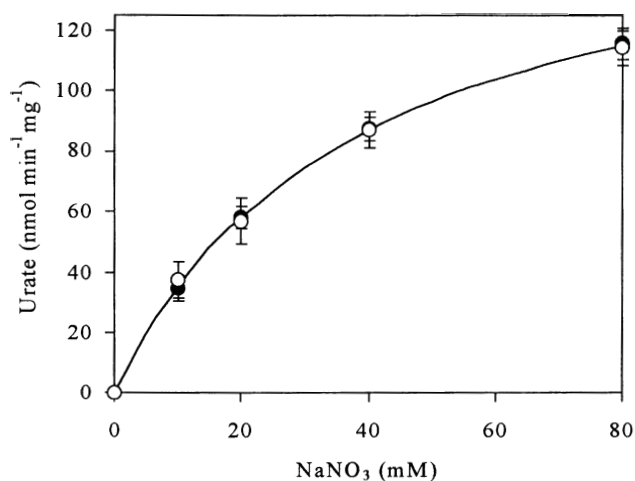


Figure 8 Xanthine oxidation in the presence of nitrate catalysed by XO and loDP-inhibited XO

The different forms of the enzyme (150 nM active subunits) were incubated under anaerobic conditions with 100 μ M xanthine and various concentrations of sodium nitrate. Data for XO (●) and loDP-inhibited XO (○) were fitted to the same Michaelis–Menten curve. Values are means \pm S.D. ($n = 3$).

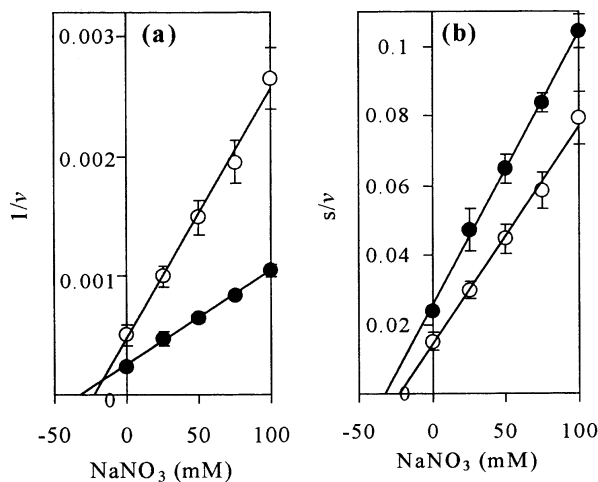


Figure 9 Inhibition by nitrate of NO production from nitrite catalysed by XO in the presence of xanthine

XO (153 nM active subunits) was incubated under anaerobic conditions with 20 μ M xanthine and various concentrations of sodium nitrate and sodium nitrite. Initial rate of NO production v is expressed in $\text{nmol} \cdot \text{min}^{-1} \cdot \text{mg}^{-1}$. (a) Dixon plot [43] of $1/v$ versus concentration of inorganic nitrate at different concentrations of sodium nitrite. (b) Cornish-Bowden plot [44] of s/v versus concentration of inorganic nitrate at different concentrations of sodium nitrite. Concentrations of sodium nitrite were 100 mM (●) and 30 mM (○). Both plots indicate predominantly competitive inhibition of nitrate against nitrite. Values are means \pm S.D. ($n = 3$).

eration of nitrite was found to follow closely that of urate, demonstrating an essentially 1:1 molar ratio between the two products at all nitrite assay points.

At least a partial explanation for the relatively very slow further reduction of nitrite to NO was provided by the demonstration that inorganic nitrate inhibits XO-catalysed reduction of nitrite (Figure 9). The predominantly competitive nature of this inhibition further supports the contention that inorganic

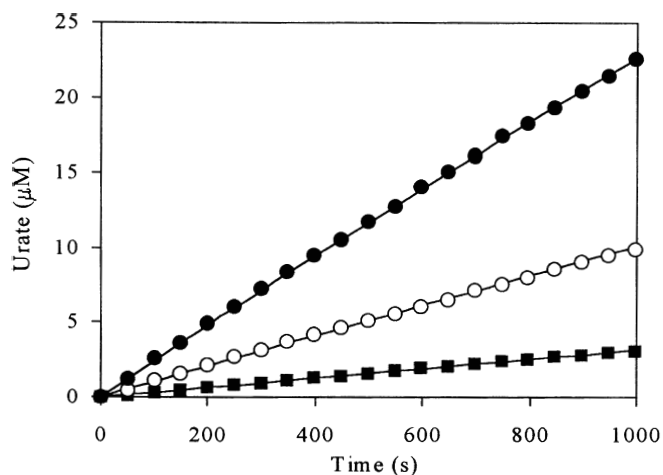


Figure 10 Progress curves of urate production catalysed by XO in the presence of xanthine and inorganic nitrate

XO (27.4 nM active subunits) was incubated anaerobically with xanthine and various concentrations of sodium nitrate: 60 mM (●), 15 mM (○) and 3.75 mM (■). Values are means from three individual progress curves. Solid lines represent fits to the model shown in Scheme 1, using the parameters shown in Table 1.

nitrate, like inorganic nitrite, acts at the molybdenum site of XOR.

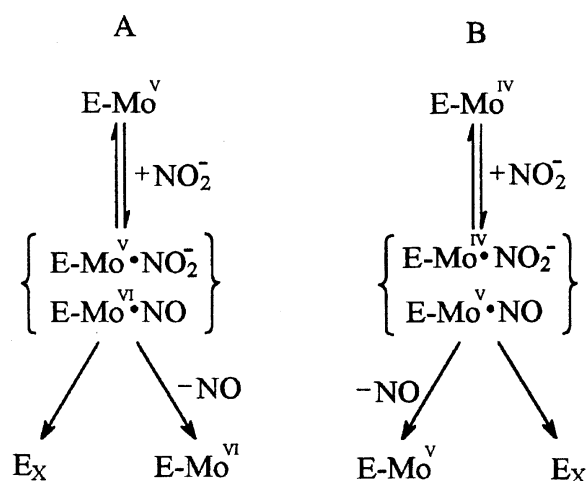
XO is not inactivated during its catalysis of nitrate reduction

In view of the above similarities, it is reasonable to propose that inorganic nitrite and nitrate interact with the molybdenum centre in an initially similar manner to form an enzyme–substrate complex. In order to assess the contribution of this phase of the reaction to enzyme inactivation, evidence for the latter was sought in the case of nitrate. Incubation of inorganic nitrate in the presence of XO and xanthine, under anaerobic conditions exactly as described for nitrite (Figure 3) showed no significant inactivation. Moreover, as can be seen in Figure 10, progress curves of XO-catalysed reduction of nitrate showed little evidence of enzyme inactivation. Fitting of the model of Scheme 1 to the progress curves led to a k_{cat}/k_1 ratio of 6103 (Table 1); a value that is an order of magnitude greater than corresponding values for nitrite, also shown in Table 1.

DISCUSSION

We reported recently that XOR is capable of catalysing the reduction of nitrite to NO under anaerobic conditions [18]. This reduction was seen to result in enzyme inactivation. Our results were in apparent agreement with reports [30,36] describing inactivation of the enzyme by exogenous NO. Because, however, these latter findings have been questioned [34,35], we sought to examine, in more detail, the mechanism of the inactivation of XOR that accompanies its catalysis of nitrite reduction.

In our earlier studies, enzyme inactivation was monitored by conventional aerobic urate assay of aliquots, taken at different time intervals, from the anaerobic reaction mixture of XO, xanthine and inorganic nitrite. After prolonged incubation, enzyme was shown to have been converted into its inactive desulpho-form, as evidenced by resulphuration (and reactivation) under standard conditions. That the inactivated enzyme, so obtained, was indeed desulpho-XO was confirmed spectrophoto-



Scheme 2 Postulated involvement of various Mo redox states of XOR in the reduction of inorganic nitrite and/or suicide inactivation

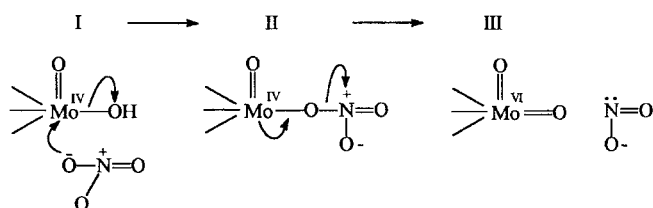
$E\text{-Mo}^{\text{IV}}$ and $E\text{-Mo}^{\text{V}}$ are those E_{R} species (Scheme 1) actively interacting with nitrite and E_{X} is the inactivated desulpho-form of the enzyme.

metrically (Figure 1). Furthermore, by monitoring absorbance at 320 nm, we have been able to demonstrate correlation of the rates of sulpho–desulpho conversion and inactivation (Figure 2), which indicates strongly that the latter directly reflects the former.

Inactivation in the above system could result either from the action of free NO on XOR, as proposed by Ichimori et al. [36], or by a suicide inactivation occurring in the enzyme–substrate/product complex. Whereas the kinetics of inactivation indicate the predominance of the latter route (Figure 3), it is difficult by these means to determine the relative contributions of the two mechanisms (see the Results section) and clarification was sought in the progress curves themselves.

Progress curves (Figure 4) of urate production in the presence of XO, xanthine and inorganic nitrite under anaerobic conditions were found to fit well to the model of Scheme 1, where K_{m} and k_{cat} are derived from the linear initial rates and k_{i} is that quoted by Ichimori et al. [36]. Good fits were similarly obtained to progress curves in the presence of XO and NADH (Figure 5) and in the presence of XDH and NADH (Figure 6). The ratio of k_{cat} to k_{i} (Table 1) can be regarded as a relative indicator of the number of productive turnovers per inactivation. Although the kinetic parameters differ for the three cases, it is noteworthy that this ratio remains reasonably independent of the nature of the reducing substrate (xanthine or NADH) or the form of the enzyme (oxidase or dehydrogenase), supporting the generality of the model. As noted in the Results section, the contribution to inactivation by free NO, based on the second-order rate constant in [36], contributed little to the overall inactivation.

The kinetic constants (Table 1) derived from fits of the model of Scheme 1 should be seen as operational parameters, rather than true rate constants. This is because the species designated E_{R} is a composite of the various reduced enzyme molecules capable of interacting productively (or destructively) with nitrite (or NO). We have demonstrated previously the 1:2 stoichiometric ratio of xanthine [20] or NADH [18] consumption to NO production in the presence of inorganic nitrite and that the latter is subjected to one-electron reduction at the Mo site [18]. Thus E_{R} may be regarded as a composite of enzyme species with Mo in its IV and V oxidation states, and the mechanism of reduction as a composite of routes A and B in Scheme 2, where $E\text{-Mo}^{\text{IV}}$



Scheme 3 Mechanism of interaction of inorganic nitrate with nitrate reductase

and $E\text{-Mo}^{\text{V}}$ are those E_{R} species actively interacting with nitrite and E_{X} is inactivated (desulpho) enzyme. However, the validity of the values of the kinetic constants is given confirmation by the observation that using these constants and the mechanism of Scheme 1 to predict the kinetics of inactivation gives fits to the data virtually identical to those shown in Figure 3.

Mechanism-based inactivation prior to release of free NO can be envisaged in several ways, one of which might involve loss of -SH groups in the course of interaction of nitrite with the molybdenum centre. While the details of this interaction are not known, analogy may be made with the assimilatory nitrate reductases, the mechanism for which is believed to essentially reverse that of the better-studied sulphite oxidase. Scheme 3 outlines such a mechanism for nitrate reductase, involving nucleophilic displacement of -OH by nitrate [4].

The reduced state of molybdenum in XOR can be portrayed analogously as species I (see Scheme 3), where either of the molybdenum-bound oxygen atoms is replaced by sulphur. Pursuing the analogy, nucleophilic displacement of an -SH group by nitrite would lead to the inactivation of XOR. Alternatively, inactivation of XOR in the course of its catalysis of nitrite reduction could result from interaction of the sulphur ligand with nascent NO prior to its release from the enzyme complex. In order to assess the contributions of these potential inactivation mechanisms the XOR-catalysed reduction of inorganic nitrate was examined.

Inorganic nitrate has been shown to be reduced to NO in the presence of NADH and XO under hypoxic conditions [46]. In the present study, we show that inorganic nitrate, like nitrite [18], is reduced at the molybdenum site of the enzyme. This, incidentally, is in contrast to organic nitrates, which act at the FAD site [47]. We also show that, in the presence of xanthine and nitrate, XO catalyses urate and nitrite production in essentially a 1:1 ratio; nitrite is presumably further reduced to NO at relatively insignificant rates in this system. The reason for such low rates of NO production may be at least partially explained in terms of competition between nitrate and nitrite for reduced enzyme.

XOR-catalysed reduction of nitrate, like that of nitrite, might be expected to be initiated by nucleophilic displacement of -SH or -OH from reduced molybdenum (see above). In so far as this displacement contributes to enzyme inactivation, it would apply equally to nitrate and nitrite. On the other hand, inactivation at a later stage, involving an intermediate enzyme–NO complex, applies primarily to reduction of nitrite, in that nitrate generates very low levels of NO and only after initial nitrite formation. In fact, incubations with nitrate showed little evidence of inactivation, as shown by both discontinuous assay and progress curves. The relative absence of enzyme inactivation with nitrate indicates that nucleophilic displacement of -SH is not occurring. This strongly suggests that a similar situation prevails in the case

of nitrite and that inactivation results from subsequent interaction of nascent NO with molybdenum-bound sulphur in the enzyme complex.

These conclusions do not contradict the findings of Ichimori et al. [36], who were studying an entirely different situation, involving inactivation of pre-reduced enzyme by relatively high concentrations of added NO. In fact, we cannot discount involvement of an analogous inactivation pathway in our system. The concentrations of free NO and consequent rates of inactivation are merely too low to make a major contribution in the course of XOR-catalysed reduction of inorganic nitrite. Indeed, our conclusion that inactivation occurs primarily at the stage of the enzyme–nitrite/–NO complex can be seen as consistent with the findings of Ichimori et al. [36], in so far as NO, in a free or complexed form, can interact with sulphur bound to a reduced form of molybdenum to give the desulpho-form of the enzyme. That this interaction should be faster when NO is directly bound in the molybdenum complex is entirely to be expected. It is likely that, in our model in Scheme 2, inactivation results from interaction of nitrite with E–Mo^{IV} and not with E–Mo^V. This would be consistent with the findings in [36] that inactivation only results when NO reacts with reduced enzyme. In Scheme 2, nascent NO is bound to a reduced form of Mo only in the E–Mo^{IV} oxidation pathway (Scheme 2, pathway B).

Inactivation of XOR in the course of nitrite reduction in the mammary gland may well serve to explain the presence of desulpho-XOR in freshly expressed milk, whether of bovine or human origin [2,7,11]. We have noted previously that XOR-catalysed generation of NO could serve a physiological function as a microbicidal agent in the neonatal gut [18,19] and similar arguments apply to the mammary gland. Supporting evidence for such a role in either location is provided by the observations that levels of XOR enzymic activity [48,49] and levels of nitrite [50] are particularly high in early *post-partum* breast milk; factors that would combine to maximize microbicidal activity.

REFERENCES

- Massey, V. and Harris, C. M. (1997) Milk xanthine dehydrogenase: the first one hundred years. *Biochem. Soc. Trans.* **25**, 750–755
- Bray, R. C. (1975) Molybdenum iron-sulfur flavin hydroxylases and related enzymes. In *The Enzymes* (Boyer, P. D., ed.), pp. 299–419, Academic Press, New York
- Patton, S. and Keenan, T. W. (1975) The milk fat globule membrane. *Biochim. Biophys. Acta.* **415**, 273–309
- Hille, R. (1996) The mononuclear molybdenum enzymes. *Chem. Rev.* **96**, 2757–2816
- Nishino, T. (1994) The conversion of xanthine dehydrogenase to xanthine oxidase and the role of the enzyme in reperfusion injury. *J. Biochem. (Tokyo)* **116**, 1–6
- Hille, R. and Nishino, T. (1995) Xanthine oxidase and xanthine dehydrogenase. *FASEB J.* **9**, 995–1003
- Harrison, R. (1997) Human xanthine oxidoreductase: in search of a function. *Biochem. Soc. Trans.* **25**, 786–791
- Harrison, R. (2000) Xanthine oxidoreductase. In *Free Radicals and Inflammation* (Winyard, P. G., Blake, D. R. and Evans, C. H., eds.), pp. 65–81, Birkhauser Press, Basel
- Bordas, J., Bray, R. C., Garner, C. D., Gutteridge, S. and Hasnain, S. S. (1980) X-ray absorption spectroscopy of xanthine oxidase. The molybdenum centres of the functional and the desulpho forms. *Biochem. J.* **191**, 499–508
- Cramer, S. P., Wahl, R. and Rajagopalan, K. V. (1981) Molybdenum sites of sulfite oxidase and xanthine dehydrogenase. A comparison by EXAFS. *J. Am. Chem. Soc.* **103**, 7721–7727
- Godber, B., Sanders, S. A., Harrison, R., Eisenthal, R. and Bray, R. C. (1997) > or = 95% of xanthine oxidase in human milk is present as the demolybdo form, lacking molybdopterin. *Biochem. Soc. Trans.* **25**, 519S
- Godber, B. L. J. (1998) Physicochemical and kinetic properties of human milk xanthine oxidoreductase, PhD Thesis, University of Bath, Bath
- Bray, R. C., Lowe, D., Godber, B., Harrison, R. and Eisenthal, R. (1999) Properties of xanthine oxidase from human milk: The enzyme is grossly deficient in molybdenum and substantially deficient in iron-sulphur centres. In *Flavins and Flavoproteins* (Ghisla, S., Kroneck, P. M. H., Macheroux, P. and Sund, H., eds.), pp. 775–778, Agency for Scientific Publication, Berlin
- Hart, L. I., McGartoll, M. A., Chapman, H. R. and Bray, R. C. (1970) The composition of milk xanthine oxidase. *Biochem. J.* **116**, 851–864
- Moncada, S. M., Palmer, R. M. J. and Higgs, E. A. (1991) Nitric oxide: physiology, pathophysiology, and pharmacology. *Pharmacol. Rev.* **43**, 109–142
- Stamler, J. S. (1994) Redox signalling: nitrosylation and related target interactions of nitric oxide. *Cell* **78**, 931–936
- Knowles, R. G. and Moncada, S. (1994) Nitric oxide synthases in mammals. *Biochem. J.* **298**, 249–258
- Godber, B. L. J., Doel, J. J., Sapkota, G. P., Blake, D. R., Stevens, C. R., Eisenthal, R. and Harrison, R. (2000) Reduction of nitrite to nitric oxide catalysed by xanthine oxidoreductase. *J. Biol. Chem.* **275**, 7757–7763
- Godber, B. L. J., Doel, J. J., Durgan, J., Eisenthal, R. and Harrison, R. (2000) A new route to peroxynitrite: a role for xanthine oxidoreductase. *FEBS Lett.* **475**, 93–96
- Doel, J. J., Godber, B. L. J., Goult, T. A., Eisenthal, R. and Harrison, R. (2000) Reduction of organic nitrites to nitric oxide catalysed by xanthine oxidase: possible role in metabolism of nitrovasodilators. *Biochem. Biophys. Res. Commun.* **270**, 880–885
- Gardner, P. R., Costantino, G., Szabo, C. and Salzman, A. L. (1997) Nitric oxide sensitivity of the aconitases. *J. Biol. Chem.* **272**, 25071–25076
- Asahi, M., Fujii, J., Suzuki, K., Seo, H. G., Kuzuya, T., Hori, M., Tada, M., Fujii, S. and Taniguchi, N. (1995) Inactivation of glutathione peroxidase by nitric oxide. Implication for cytotoxicity. *J. Biol. Chem.* **270**, 21035–21039
- Cleeter, M. W., Cooper, J. M., Darley-Usmar, V. M., Moncada, S. and Schapira, A. H. (1994) Reversible inhibition of cytochrome c oxidase, the terminal enzyme of the mitochondrial respiratory chain, by nitric oxide. Implications for neurodegenerative diseases. *FEBS Lett.* **345**, 50–54
- Brown, G. C. and Cooper, C. E. (1994) Nanomolar concentrations of nitric oxide reversibly inhibit synaptosomal respiration by competing with oxygen at cytochrome oxidase. *FEBS Lett.* **356**, 295–298
- Fujii, H., Ichimori, K., Hoshiai, K. and Nakazawa, H. (1997) Nitric oxide inactivates NADPH oxidase in pig neutrophils by inhibiting its assembling process. *J. Biol. Chem.* **272**, 32773–32778
- Galley, H.-F., Davies, M. J. and Webster, N. R. (1996) Xanthine oxidase activity and free radical generation in patients with sepsis syndrome. *Crit. Care Med.* **24**, 1649–1653
- Grum, C. M., Ragsdale, R. A., Ketai, L. H. and Simon, R. H. (1987) Plasma xanthine oxidase activity in patients with adult respiratory distress syndrome. *J. Crit. Care* **2**, 22–26
- Akaike, T., Ando, M., Oda, T., Doi, T., Iijri, S., Araki, A. and Maeda, H. (1990) Dependence on O₂⁻ generation by xanthine oxidase of pathogenesis of influenza virus infection in mice. *J. Clin. Invest.* **85**, 739–745
- Wang, P. and Zweier, J. L. (1996) Measurement of nitric oxide and peroxynitrite generation in the postischemic heart. Evidence for peroxynitrite-mediated reperfusion injury. *J. Biol. Chem.* **271**, 29223–29230
- Fukahori, M., Ichimori, K., Ishida, H., Nakagawa, H. and Okino, H. (1994) Nitric oxide reversibly suppresses xanthine oxidase activity. *Free Radical Res.* **21**, 203–212
- Rinaldo, J. E., Clark, M., Parinello, J. and Shepherd, V. L. (1994) Nitric oxide inactivates xanthine dehydrogenase and xanthine oxidase in interferon-gamma-stimulated macrophages. *Am. J. Resp. Cell Mol. Biol.* **11**, 625–630
- Hassoun, P. M., Yu, F. S., Zulueta, J. J., White, A. C. and Lanzillo, J. J. (1995) Effect of nitric oxide and cell redox status on the regulation of endothelial cell xanthine dehydrogenase. *Am. J. Physiol.* **268**, L809–L817
- Cote, C. G., Yu, F. S., Zulueta, J. J., Vosatka, R. J. and Hassoun, P. M. (1996) Regulation of intracellular xanthine oxidase by endothelial-derived nitric oxide. *Am. J. Physiol.* **271**, L869–L874
- Houston, M., Chumley, P., Radi, R., Rubbo, H. and Freeman, B. A. (1998) Xanthine oxidase reaction with nitric oxide and peroxynitrite. *Arch. Biochem. Biophys.* **355**, 1–8
- Lee, C. I., Liu, X. and Zweier, J. L. (2000) Regulation of xanthine oxidase by nitric oxide and peroxynitrite. *J. Biol. Chem.* **275**, 9369–9376
- Ichimori, K., Fukahori, M., Nakazawa, H., Okamoto, K. and Nishino, T. (1999) Inhibition of xanthine oxidase and xanthine dehydrogenase by nitric oxide. *J. Biol. Chem.* **274**, 7763–7768
- Massey, V., Komai, H., Palmer, G. and Elion, G. (1970) On the mechanism of inactivation of xanthine oxidase by allopurinol and other pyrazolo[3,4-d]pyrimidines. *J. Biol. Chem.* **245**, 2837–2844
- Avis, P. G., Bergel, F. and Bray, R. C. (1956) Cellular constituents. The chemistry of xanthine oxidase. Part III. Estimations of the cofactors and the catalytic functions of enzyme fractions from cows' milk. *J. Chem. Soc.* , 1219–1225
- O'Donnell, V. B., Smith, G. C. M. and Jones, O. T. G. (1994) Involvement of phenyl radicals in iodonium inhibition of flavoenzymes. *Mol. Pharmacol.* **46**, 778–785

-
- 40 Horecker, B. L. and Kornberg, A. (1948) The extinction coefficients of the reduced band of pyridine nucleosides. *J. Biol. Chem.* **175**, 385–390
- 41 Beckman, J. S., Parks, D. A., Pearson, J. D., Marshall, P. A. and Freeman, B. A. (1989) A sensitive fluorometric assay for measuring xanthine dehydrogenase and oxidase in tissues. *Free Radical Biol. Med.* **6**, 607–615
- 42 Griess, P. (1879) Bemerkungen zu der Abhandlung der HH. Weselsky und Benedikt 'Ueber einige Azoverbindungen' *Berichte der Deutschen Chemische Gesellschaft* **12**, 426–429
- 43 Dixon, M. (1953) The determination of enzyme inhibitor constants. *Biochem. J.* **55**, 170–171
- 44 Cornish-Bowden, A. (1974) A simple graphical method for determining the inhibition constants of mixed, uncompetitive and non-competitive inhibitors. *Biochem. J.* **137**, 143–144
- 45 Massey, V. and Edmondson, D. (1970) On the mechanism of inactivation of xanthine oxidase by cyanide. *J. Biol. Chem.* **245**, 6595–6598
- 46 Millar, T. M., Stevens, C. R., Benjamin, N., Eisenthal, R., Harrison, R. and Blake, D. R. (1998) Xanthine oxidoreductase catalyses the reduction of nitrates and nitrite to nitric oxide under hypoxic conditions. *FEBS Lett.* **427**, 225–228
- 47 Doel, J. J., Godber, B. L. J., Eisenthal, R. and Harrison, R. (2001) Reduction of organic nitrates catalysed by xanthine oxidoreductase under anaerobic conditions. *Biochim. Biophys. Acta* **1527**, 81–87
- 48 Brown, A.-M., Benboubetra, M., Ellison, M., Powell, D., Reckless, J. D. and Harrison, R. (1995) Molecular activation-deactivation of xanthine oxidase in human milk. *Biochim. Biophys. Acta* **1245**, 248–254
- 49 Stevens, C. R., Millar, T. M., Clinch, J. G., Kanczler, J. M., Bodamyali, T. and Blake, D. R. (2000) Antibacterial properties of xanthine oxidase in human milk. *Lancet* **356**, 829–830
- 50 Iizuka, T., Sasaki, M., Oishi, K., Uemura, S., Koike, M. and Shinozaki, M. (1999) Non-enzymatic nitric oxide generation in the stomachs of breastfed neonates. *Acta Paediatr.* **88**, 1053–1055
-

Received 1 December 2000/8 June 2001; accepted 25 June 2001